Analysis of the Effect of Temperature on the Wideband Characteristics of EMI Filters

Dong Chao*, Chen Han, and Mingxing Du

Abstract—This paper analyzes the variation trend of transmission coefficients of two electromagnetic interference filters with different structures in different temperature environments. Considering the influence of mutual-inductance between capacitors and temperature on parasitic parameters, we construct a wideband equivalent circuit model of electromagnetic interference filter and calculate the coefficient of the parameter as a function of temperature by measuring the parasitic parameters of common mode chokes (CMC) in different temperature environments. Because the wide range of selected temperature changes, it is necessary to divide the entire temperature range into two temperature segments and calculate the temperature coefficients respectively to ensure the accuracy of the data. Through the simulation and experiment, we have obtained the variation trend of the transmission coefficient of two kinds of structural electromagnetic interference filters under different temperature environments, and the trend shows that the attenuation performance of the filter rises first and then decreases with the increase of temperature, which verifies that the temperature will affect the performance of the filter.

1. INTRODUCTION

At present, filters are widely used in electronic products to deal with electromagnetic interference (EMI) problems. For instance, some products have power lines connected to EMI filters to suppress conducted EMI, which meet the requirements of national standards for electromagnetic compatibility [1]. Filters consisting of passive components such as capacitors and inductors have a good suppress to conduct EMI. However, its parasitic parameters or the nature of the material itself are susceptible to a variety of factors, such as thermal problems due to product loss, causing changes in the temperature of the working environment. The ambient temperature affects the value of the parasitic parameters of the passive components, which in turn affects the performance of the filter [2].

In high-frequency conditions, the performance of the capacitor is usually affected by parasitic effects, and the self-inductance and mutual inductance of each component are affected by changes in ambient temperature [3, 4]. For an inductor, temperature changes affect the magnetic permeability of the core, which in turn changes its inductance [5]. Temperature affects the performance of passive components, which will have an important impact on EMI filters composed of passive components. Therefore, it is important to study the temperature dependence of EMI filters.

Capacitance and inductance are the key components of EMI filters. Modeling can be used to analyze the effects of temperature on capacitance and inductance, which predict the behavior of filter performance with temperature. To this end, this paper is devoted to the construction of models of passive components and filters in accordance with actual operating conditions and to study the general

method for accurately characterizing and measuring parasitic parameters in the constructed model [6–10]. A simple measurement method for the CMC transmission coefficient is proposed in [11]. This method connects one of the windings of the CMC to the vector network analyzer (VNA) and the other windings to open circuit. This open circuit structure characterizes the common mode attenuation ability provided by the CMC in the low frequency part, and the differential mode attenuation ability of the coupling inductance in the high frequency part. The performance of the CMC can be predicted quickly with a very simple circuit.

Ref. [12] proposed two filter structures of parallel capacitors and anti-parallel capacitors, analyzed the self-inductance and mutual inductance effects of capacitors, and studied the transmission coefficients of the two topologies. Based on these two topological structures, we have deeply studied the variation of parasitic parameters of CMC in different temperature environments and calculated its temperature coefficient. We use the software Pspice to simulate the wideband characteristics of the two topology filters under different temperature conditions. Then we build two test circuits and measure the filter transmission coefficient under five temperature conditions with vector network analyzer, compare them with the simulation results, and verify the relationship between the attenuation performance of the filter and the temperature.

2. MODELING OF CAPACITOR AND COMMON MODE CHOKE

The most appropriate electrical model for real capacitors has three to four electrical elements. The complex circuit can be simplified by removing the parasitic elements that have a negligible impact on the global performance of the component. ESR, ESL, and C are the main elements of a capacitor. In the equivalent circuit of a device, the temperature dependence of these three parameters needs to be considered. A typical capacitive wideband equivalent model can be used to describe the behavior of the measured capacitor over temperature and over a wideband range, as shown in Fig. 1. The equivalent series inductance approximates a constant under different temperature conditions, and only C and ESR vary with temperature [7]. These data can be provided by the supplier of the component.

Figure 1. Capacitor circuit model.

A common technique employed to increase the high frequency attenuation of EMI filters is to place two capacitors in parallel. In principle, the equivalent inductance of two equal capacitors in parallel will be one half of that of a single capacitor, thus increasing the attenuation at high frequencies compared with the case of a single capacitor. However, this simple calculation disregards the impact of mutual inductance between capacitors, which might undermine the expected improvement. Fig. 2 shows the different connection structures of the two capacitors, called parallel structure and anti-parallel structure. The distance between the capacitors of the two connection structures is 0.5 mm, and currents in parallel structure capacitors flow in the same direction, whereas in the other case, currents flow in opposite directions. The key difference between these two structures is the mutual inductance between the capacitors, the mutual inductance between the parallel structure capacitors can be neglected, and the mutual inductance of the anti-parallel structure cannot be ignored. Because the mutual inductance between the capacitors reduces their total inductance, the high-frequency performance of the anti-parallel filter is better than the parallel structured filter [12]. Also, another important difference between these two arrangements is that the trace between the two capacitors will be typically larger in the anti-parallel case, yielding a higher parasitic inductance, L_d. Note that in spite of the small value of L_d, it may have a significant impact on the performance of the filter at high frequencies because it is placed between the two capacitors. Therefore, the shortest connection line should be made when wiring [13].

The common mode choke has two windings, which can be regarded as a four-port network, as shown in Fig. 3, and this model divides the coupling inductance into common mode (CM) and differential mode (DM), including the inductance L_{CM}, L_{DM} of the winding. In addition, the parasitic capacitance of
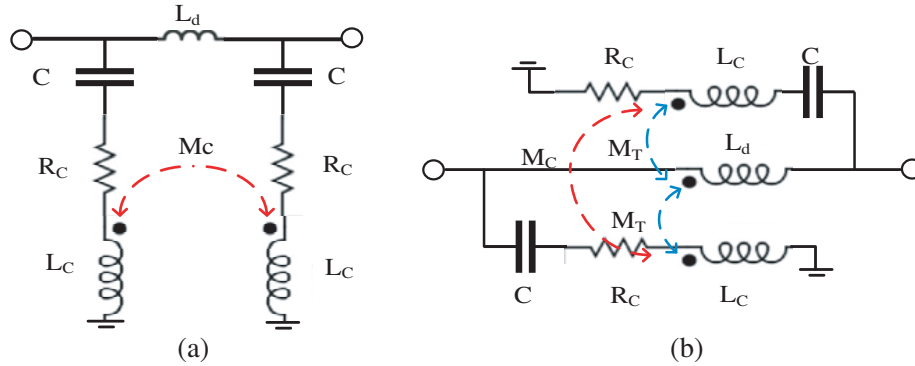
Figure 2. Capacitor connection structure. (a) Parallel arrangement, and (b) anti-parallel arrangement.
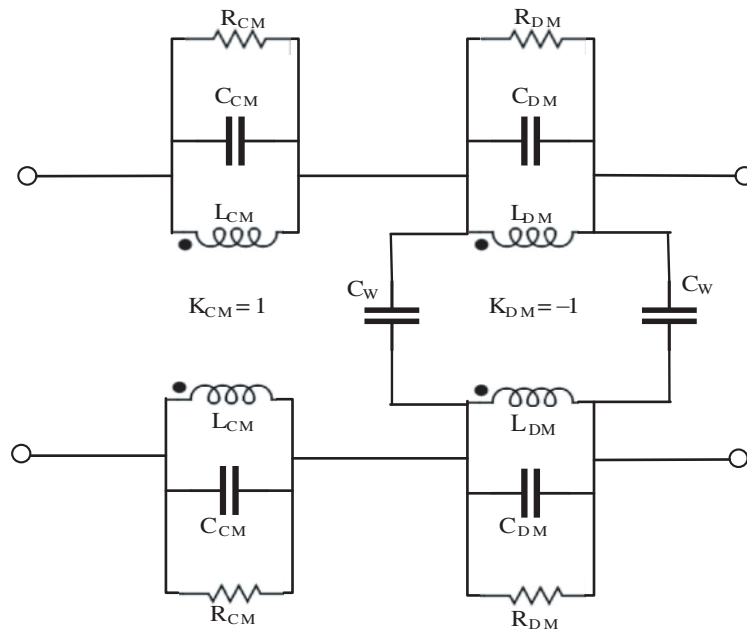
Figure 3. Wideband equivalent circuit model of common mode choke.

single-end winding C_{CM}, C_{DM} and parasitic capacitance C_W between the windings at both ends, and the self-resistance R_{CM}, R_{DM} of CMC are added.

The model has two advantages: First, it clearly shows the parasitic parameters that affect the CM and DM currents in the CMC. For instance, it shows that the capacitor C_W has no effect on the CM current, but L_{CM} affects the CM current, and the inductor L_{DM} acts on the DM current. Second, it is easy to consider the frequency characteristics of the parasitic parameters in the model. Since the inductance of the CMC varies with frequency, it is necessary to treat L_{CM} and L_{DM} as two independent parameters [12]. k is the ideal coupling coefficient, $k = 1$ the CM part, and $k = -1$ the DM part.

3. MEASUREMENT OF PARASITIC PARAMETERS AND CALCULATION OF TEMPERATURE COEFFICIENT

The effect of temperature on filter performance is essentially the influence on parasitic parameters of the filter, which can be measured with a precision impedance analyzer. In order to determine the various parasitic parameters of the model and their values in different temperature environments, three measurement methods are needed to measure different parameters. A 2.2 mH CMC with a core material

(a)   (b)

(c)
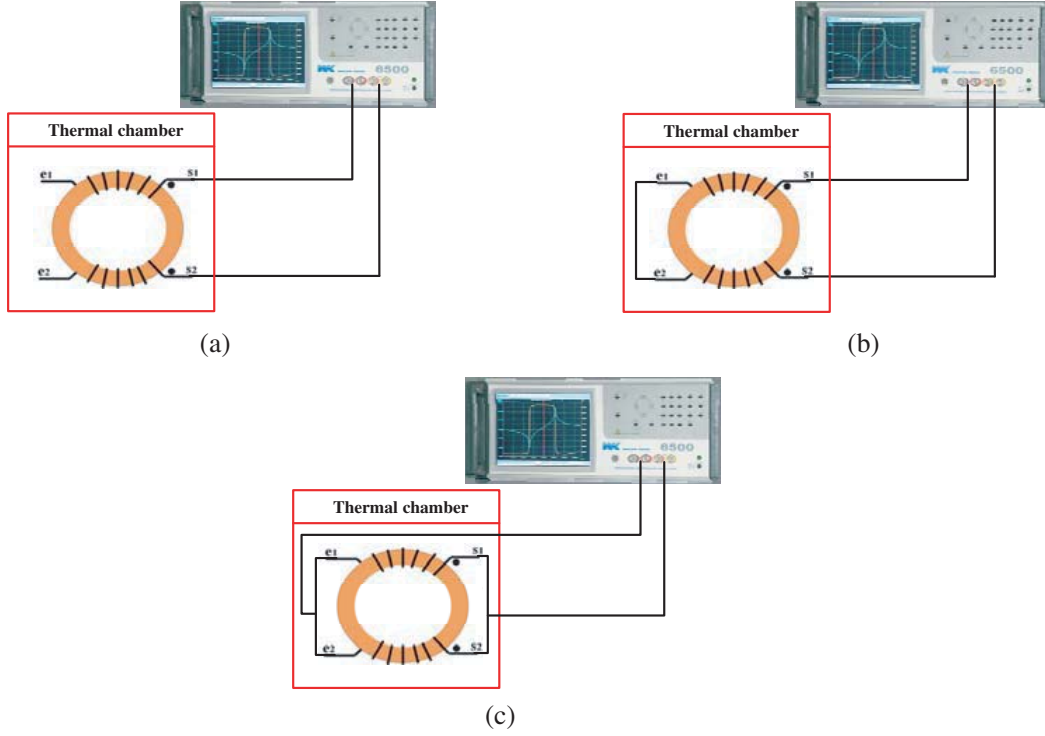
Figure 4. Measurement configurations of common mode choke under temperature variations. (a) Method for measuring parasitic parameter C_W, and (b) method for measuring differential mode parasitic, and (c) method for measuring common mode parasitic parameters.

of manganese-zinc is mounted on the filter. The measured frequency range is 100 KHz–50 MHz, as shown in Fig. 4, (a) measures the parasitic capacitance C_W between the windings of the CMC; (b) measures the DM parasitic parameters; (c) measures the CM parasitic parameters. A thermal chamber is used to change the ambient temperature of the component under test (10°C–80°C).

The parasitic capacitance C_W between two windings of CMC is calculated through the following formula:

$$C_w = \frac{1}{2}C_{Wm} \tag{1}$$

The DM parasitic parameters of the CMC are calculated through the following formula:

$$L_{DM} = \frac{1}{2}L_{DMm} \tag{2}$$

$$R_{DM} = \frac{1}{2}R_{DMm} \tag{3}$$

$$C_{DM} = 2\left(C_{DMm} - C_W\right) \tag{4}$$

where C_{Wm}, R_{DMm}, C_{DMm} are measured values.

Parasitic parameter values of the CMC at five ambient temperatures are shown in Table 1 and Table 2.

It can be seen from Table 1 and Table 2 that the parasitic parameters of the CMC have different trends before and after 40°C, and the value of the inductor rises before 40°C and decreases after 40°C. This is related to the core material of CMC. In order to improve the accuracy of the simulation, the temperature coefficients of the parasitic parameters at 10°C–40°C and 40°C–80°C are calculated, respectively. The data of temperature coefficients of capacitors can be obtained by the supplier.

The temperature coefficients are calculated through the following formula:

$$T_{c1} + T_{c2}\left(T - T_0\right)^2 = \frac{X - X_0}{X_0\left(T - T_0\right)} \tag{5}$$

Table 1. Common mode choke common mode parasitic parameters.

Parameter	10°C	20°C	40°C	65°C	80°C
L_{CM} (mH)	3.535	3.765	4.235	4.125	4.275
R_{CM} (kΩ)	6.335	6.475	6.525	5.595	5.085
C_{CM} (pF)	6.2	6.37	6.63	6.57	6.64

Table 2. Differential mode choke common mode parasitic parameters.

Parameter	10°C	20°C	40°C	65°C	80°C
L_{DM} (mH)	4.672	4.68	4.72	4.713	4.733
R_{DM} (kΩ)	7.625	7.425	6.975	6.32	6.11
C_{DM} (pF)	2.75	2.785	2.815	2.985	3
C_W (pF)	3.87	3.885	3.915	3.97	4.01

where T_{c1} and T_{c2} are linear temperature coefficient and secondary temperature coefficient, respectively; T_0 is the initial temperature; X_0 is the parasitic parameter value at the initial temperature; T is the temperature after the change; and X is the parasitic parameter value after the temperature change. The formula is applied to the calculation of the temperature coefficient of all parasitic parameters.

4. WIDEBAND CHARACTERISTICS OF FILTERS UNDER THE VARIETY OF TEMPERATURES

In order to evaluate the advantages of the anti-parallel structure of the capacitors in the SC filter, we construct two SC filter test boards. The two filters occupy the same space in the test circuit, and each pair of capacitors is connected in parallel, but the track of the capacitor connection is different, as shown in Fig. 5. The anti-parallel layout design in Fig. 5(b) causes mutual coupling between each pair of capacitors, and current flows in opposite directions in each pair of capacitors. The high frequency model of the filter is shown in Fig. 6. In this paper, the common mode capacitor (Y) value is 10 nF; the differential mode capacitor (X) value is 150 nF; and both capacitors are TENTA thin-film capacitors. The parameters of the model are shown in Table 3 [12].

The common mode (CM) transmission coefficient measurement and simulation results of the two SC filters are shown in Fig. 7(a). Note that the filter with an anti-parallel structure outperforms the filter with a parallel structure by approximately 7 dB at high frequencies. It must be highlighted that this improvement is obtained with no increase of the cost, weight, or the space required by the filter. Also, note that the measured and simulated curves exhibit an excellent agreement, which demonstrates
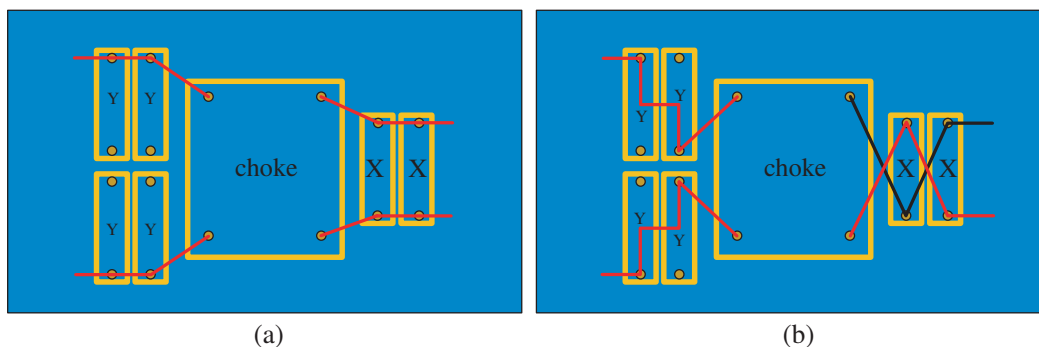
Figure 5. Shunt-capacitor filter layout. (a) Parallel structure, and (b) anti-parallel structure.
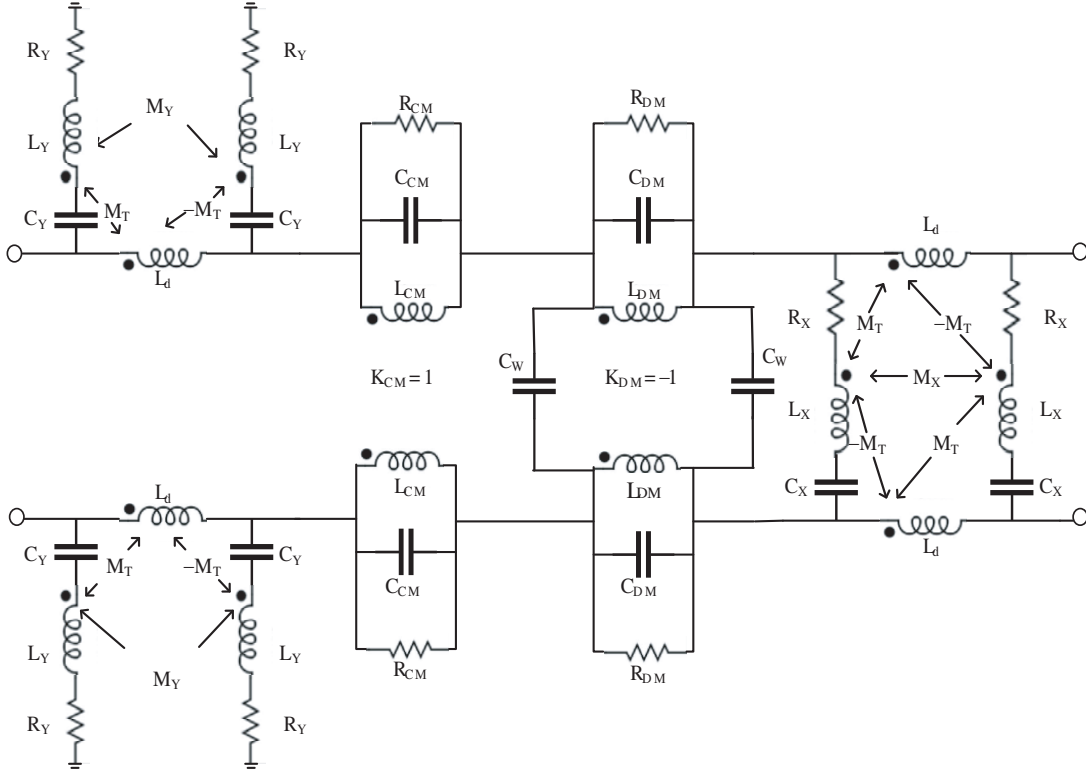
Figure 6. High frequency model of filter.

Table 3. Model parameters of filter high ferquency circuit.

Coupled inductance		Capacitor		
Parameter	Value	Parameter	Parallel	Anti-parallel
L_{CM}	4 mH	C_X/C_Y	0.15 uF/0.01 uF	
L_{DM}	4.7 uH	$w \times h \times t \times p$	C_X: $18 \times 14.5 \times 8.5 \times 15$ (mm)	
R_{CM}	6.5 kΩ		C_Y: $13 \times 11 \times 5 \times 10$ (mm)	
R_{DM}	7.2 kΩ	L_X/L_Y	12 nH/25 nH	
C_{CM}	6.5 pF	R_X/R_Y	75 mΩ/143 mΩ	
C_{DM}	2.8 pF	L_D	0	4.3 nH
C_W	3.9 pF	$M_X/M_Y/M_T$	0	$-4.2/-4.2/2.9$(nH)

that the effect of the mutual coupling between the Y-capacitors accounts for a better performance of the filter with anti-parallel coupling (X-capacitors are ineffective for CM signals).

Figure 7(b) compares the transmission coefficients of two SC filters for a differential mode (DM) signal and gives the measurement and simulation results. Measured and simulated results depicted in that figure reveal that also in this case, the anti-parallel arrangement of the capacitors provides an advantage in terms of attenuation at high frequencies (improvements between a few decibels and 8 dB above 6 MHz). However, simulated S_{21} curves with the circuit model of Fig. 6 and the parameters in Table 3 do not agree well with the measured results at high frequencies. This makes a stark contrast with the CM case in Fig. 7(a), where concordance between the measured and simulated results is much better. The difference observed in the DM case is due to the effect of mutual coupling between the CMC and capacitors, which is a much more important effect for a DM signal than for a CM signal [11, 14].
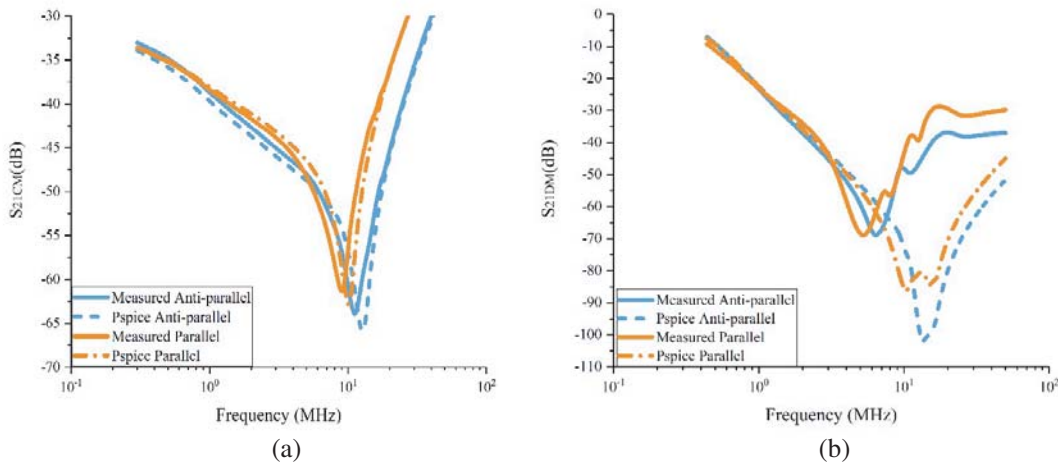
Figure 7. Transmission coefficient of SC filters. (a) Common mode, and (b) differential mode.
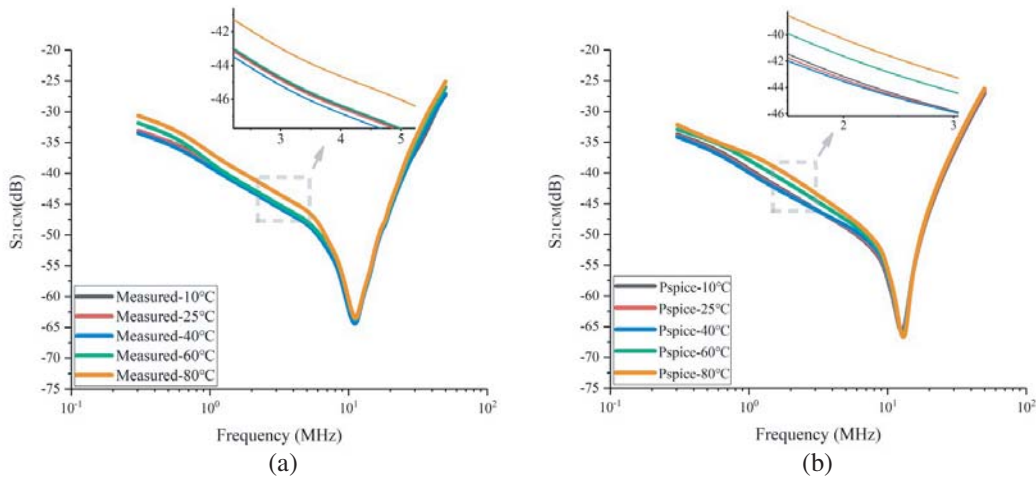
Figure 8. Transmission coefficients of anti-parallel structure filter at various temperatures. (a) Measurement result, and (b) simulation result.

In order to improve the simulation accuracy of the DM signal attenuation in the SC filter, the mutual coupling effect between the CMC and capacitor should be considered and included in the circuit model of Fig. 6, which is not included in this paper.

Figure 8 compares the measurement and simulation results of the common mode (CM) transmission coefficient of the anti-parallel SC filter under variety of temperature conditions. It can be seen from Fig. 8(a) that before the resonant frequency, S_{21} value shows a trend of first rising and then falling with the rise of temperature, and $40°C$ is the inflection point of trend change which is consistent with the inflection point of inductance value changing with temperature in Table 1 and Table 2. The S_{21} value after the resonant frequency value and the resonant frequency does not change significantly, and the maximum difference between different temperatures does not exceed 0.3 dB. It can be concluded that the common mode attenuation performance of the anti-parallel structure filter rises first and then decreases before the resonance frequency, with $40°C$ as the inflection point. However, the attenuation performance change at the resonance point is not obvious In addition, the curves of the measurements and simulations show good agreement.

Figure 9 compare the measurement and simulation results of the common mode (CM) transmission coefficient of the parallel structure SC filter under the variety of temperatures. It can be seen from Fig. 9 that the S_{21} value rises first and then decreases with the increase of temperature before the
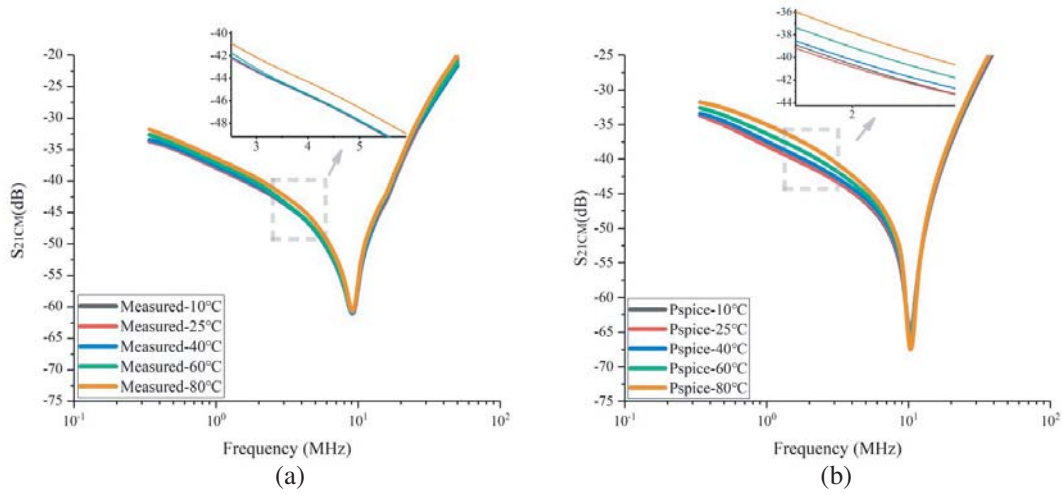
Figure 9. Transmission coefficients of parallel structure filter at various temperatures. (a) Measurement result, and (b) simulation result.

resonance frequency, with 25°C as the inflection point, and the inflection point has a certain gap with the temperature inflection point of 40°C of the inductance values in Table 1 and Table 2. The S_{21} value after the resonant frequency value and the resonant frequency does not change significantly, and the maximum difference between different temperatures does not exceed 0.6 dB. It can be concluded that the common mode attenuation performance of the parallel structure filter rises first and then decreases before the resonance frequency, taking 25°C as the inflection point, and the attenuation performance change at the resonance point is not obvious. The curves of measurements and simulations show good agreement.

From the experimental and simulated results, it can be concluded that the overall trend of attenuation performance of both parallel structure filters and anti-parallel structure filters will rise first and then decrease with the increase of temperature, but the inflection points of different structural filters are different.

5. CONCLUSIONS

In order to accurately characterize the wideband characteristics of SC filters under different temperature conditions, we have studied the measurement of the parasitic parameters of the filter components and the calculation method of the temperature coefficient, and constructed a simulation model of the SC filter under the Pspice software platform. The wideband characteristics of SC filters in different temperature environments are predicted by the simulation model. Through the comparison of experiment and simulation results, the high-frequency performance of the anti-parallel structure filter is better than the parallel one, and the common mode measurement results are in good agreement with the simulation ones. However, the measurement of differential mode is not consistent with the simulation results, which will be our future work direction. In addition, by analyzing the transmission coefficient of the filter in different temperature environments, we have obtained the relationship between the filter attenuation performance and the temperature.

REFERENCES

1. Paul, C. R., *Introduction to Electromagnetic Compatibility*, Wiley, Hoboken, NJ, USA, 2006.

2. Negrea, C., M. Rangu, and P. Svasta, "SPICE modeling of thermal behavior for passive components," *International Spring Seminar on Electronics Technology*, 486–491, IEEE, 2011.

3. Wang, S., F. C. Lee, and W. G. Odendaal, "Cancellation of capacitor parasitic parameters for noise reduction application," *IEEE Transactions on Power Electronics*, Vol. 21, No. 4, 1125–1132, 2006.

4. Kovacevic, I. F., et al., "3-D electromagnetic modeling of parasitics and mutual coupling in EMI filters," *IEEE Transactions on Power Electronics*, Vol. 29, No. 1, 135–149, 2014.

5. Yu, X., "Research on the relationship of power line filter's performance and factors such as temperature and techniques of anti-saturation," M.Sc. Dissertation, Department of Mechanical Engineering, Southeast University, Nanjing, China, 2017 (in Chinese).

6. Kotny, J. L., X. Margueron, and N. Idir, "High-frequency model of the coupled inductors used in EMI filters," *IEEE Transactions on Power Electronics*, Vol. 27, No. 6, 2805–2812, 2012.

7. Hami, F., H. Boulzazen, and M. Kadi, "High-frequency characterization and modeling of EMI filters under temperature variations," *IEEE Transactions on Electromagnetic Compatibility*, Vol. 59, No. 6, 1906–1915, 2017.

8. Kotny, J. L., T. Duquesne, and N. Idir, "EMI filter design using high frequency models of the passive components," *IEEE Workshop on Signal Propagation on Interconnects*, 143–146, 2011.

9. Hami, F., H. Boulzazen, and M. Kadi, "Wideband characterization and modeling of coupled inductors under temperature variations," *IEEE International Symposium on Electromagnetic Compatibility*, 1394–1401, IEEE, 2015.

10. Chen, H. F., C. Y. Yeh, and K. H. Lin, "A method of using two equivalent negative inductances to reduce parasitic inductances of a three-capacitor EMI filter," *IEEE Transactions on Power Electronics*, Vol. 24, No. 12, 2867–2872, 2009.

11. Dominguez-Palacios, C., J. Bernal, and M. M. Prats, "Characterization of common mode chokes at high frequencies with simple measurements," *IEEE Transactions on Power Electronics Electronics*, Vol. 33, No. 5, 3975–3987, 2018.

12. Gonzalez-Vizuete, P., F. Fico, A. Fernandez-Prieto, M. J. Freire, and J. Bernal Mendez, "Calculation of parasitic self- and mutual-inductances of thin-film capacitors for power line filters," *IEEE Transactions on Power Electronics*, Vol. 34, No. 1, 236–246, 2019.

13. Bernal, J., M. Freire, and S. Ramiro, "Simple and cost-effective method for improving the high frequency performance of surface-mount shunt capacitors filters," *IEEE International Symposium on Electromagnetic Compatibility*, 372–377, IEEE, 2015.

14. Chen, H. and Z. Qian, "High frequency modeling for common mode chokes based on impedance measurement," *Transactions of China Electrotechnical Society*, Vol. 22, No. 4, 8–12, 2007 (in Chinese).